2018

Investigating phosphorylation patterns and their effect on the activity of transcription factor TaABF1 in imbibing cereal grains

Grace Uwase
Colby College

Investigating phosphorylation patterns and their effect on the activity of transcription factor TaABF1 in imbibing cereal grains

By
Grace Uwase

A Thesis Presented to the Department of Chemistry,
Colby College, Waterville, ME
In Partial Fulfillment of the Requirements for Graduation
With Honors in Chemistry

Submitted May 2018

Investigating phosphorylation patterns and their effect on the activity of transcription factor TaABF1 in imbibing cereal grains

By
Grace Uwase

Approved:

_____

(Mentor. Russell R. Johnson, Professor of Biology)

_____Date

_____

(*Reader. Kevin P. Rice, Associate Professor of Chemistry)*

_____Date

TABLE OF CONTENTS

Abstract

The wheat transcription factor TaABF1 plays an important role in hormone-mediated regulation of seed dormancy and germination of cereal grains. Evidence shows that TaABF1 activity is regulated by phosphorylation, and previous work in our lab showed that when serine residues in its conserved regions (S36, S37, S113, S115) were altered to the phosphomimetic amino acid aspartate, the 4xD TaABF1 mutant had increased activity as a transcription factor. However, when only S113 was altered, TaABF1's activity was greatly reduced. The work presented here explored whether the S36D/S37D/S115D mutant would have stronger activity than the 4xD mutant. Using the particle bombardment technique to introduce the TABF1 effector and reporter constructs in aleurone cells, we found that the 3xD mutant was able to enhance TaABF1 activity, but not to a stronger degree than the 4xD. This suggest that the phosphorylation effect of these residues is not additive, and individual residues have different roles in regulating TaABF1 activity. We also complemented this work by attempting to identify TaABF1 phosphorylation sites in untreated wheat grains by exposing purified TaABF1 to aleurone kinases and analyzing the resulting phosphorylation patterns using LC-MS/MS. We successfully detected phosphorylatable TaABF1 peptides at high intensities, but we did not detect any TaABF1 phosphopeptides. Determining sites of TaABF1 phosphorylation under different conditions will give insights in what role specific residues play in regulating TaABF1 activity, as well as the TaABF1 mechanism of action in regulating the ABA and GA pathways in imbibing cereal grains.

Introduction

Throughout its lifetime, a plant uses various mechanisms to properly respond to environmental stimuli. In cereal grain development, the hormones abscisic acid (ABA) and gibberellin (GA) have opposing effects to regulate development and modulate response to environmental conditions. ABA was first isolated in 1963, and was initially believed to accelerate abscission of plant organs (Ohkuma *et al.*, 1963). Later studies showed that ABA was not directly involved in the abscission process, but rather promoted senescence and stress responses preceding abscission (Sah *et al*., 2016). It is currently widely understood that abiotic stresses such as drought, high salinity, and extreme temperatures can trigger the ABA biosynthetic pathway. The presence of ABA can then lead to a variety of responses, ranging from physical responses such as stomatal closure to changing gene expression patterns that promote adaptive responses (Miyakawa *et al*., 2013; Sah *et al*., 2016).

For ABA perception and signaling, due to its hydrophobic structure (Fig. 1), ABA receptors can be transmembrane, soluble in the cytoplasm, and/or the nucleus (Finkelstein *et al*., 2002). Although much work is still being done to understand the ABA pathway, the core signaling complexes that perceive ABA and initiate signal transduction have been identified. The ABA response involves ABA receptors (**ABAR**, also known as Pyrabactin Resistance [PYR], PYR1-Like [PYL], or Regulatory Component of ABA Receptor [RCAR]), group-A protein phosphatases 2C (**PP2C**), and subclass III sucrose nonfermenting-1 (SNF1)-related protein kinase 2 (**SnRK2**) (Miyakawa *et al*., 2013). ABA binds to ABAR and forms a ternary complex with PP2Cs in which the phosphatase activity of PP2C is inhibited. This enables autophosphorylation and activation of SnRK2s, which can lead to ABA-induced stomatal closure through the targeting of NADPH oxidases and ion channels. SnRK2 activation also leads to ABA-mediated transcriptional regulation through the activation of basic leucine zipper (**bZIP**) transcription factors, such as ***A***BA-responsive

element (**ABRE**) ***B***inding ***F***actors (**ABFs**). ABREs contain the consensus sequence (T/C)ACGTGGC. ABFs then bind and regulate promoters that contain ABRE and a coupling element containing the consensus sequence CGCGTG (Johnson *et al*., 2002). Genome-wide transcriptome analysis of *Arabidopsis* with mutations in four ABF genes; *areb1, areb2, abf1,* and *abf3,* indicated that these transcription factors regulate a wide range of genes involved in drought and osmotic stress response and tolerance. The mutant plants displayed lower survival rates upon exposure to drought stress compared to wild type, and the primary root growth of the mutant plants was significantly less inhibited by ABA (Yoshida *et al*., 2015). These experiments support the role of ABFs in the ABA-response pathway.

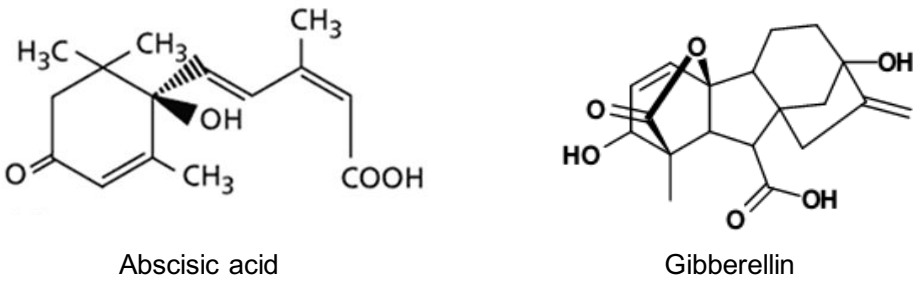

Abscisic acid Gibberellin

Figure 1. Molecular structures of abscisic acid and gibberellin A_3

The role of ABA in plants also includes functions such as modulation of root architecture, stomata regulation, and various contributions to seed development (Sah *et al*., 2016). In developing seeds, ABA can either be derived from maternal tissues or be synthesized *de novo* in the embryo. Maternally-derived ABA has been shown to accumulate about halfway during seed development and promotes the synthesis of storage proteins. During seed imbibition, *de novo* ABA biosynthesis in the embryo is a determinant of seed dormancy. Dormant seeds are unable to germinate, even when the conditions for germination are favorable. This confers ecological advantages such as ensuring that germination only occurs when chances of survival are high, as well as preventing pre-

harvest sprouting. Seed dormancy and germination are under genetic control regulated by a dynamic balance between ABA and GA. In contrast to non-dormant seeds, dormant barley grains were found to have a higher concentration of endogenous ABA, showed increased *de novo* ABA synthesis, and they were more sensitive to exogenous ABA (Wang *et al*., 1995; Rodríguez-Gacio *et al*., 2009).

In wheat and barley, GA is released from the embryo and sent to the aleurone cells, where it induces the expression of various genes involved in promoting growth. In early 1900s, a disease known as the "foolish seedling disease" caused rice plants to grow taller with lowered seed production, but was later found to occur when the rice was infected by a GA- producing fungus. GA is now understood to be an endogenous plant growth regulator, found in actively growing tissue such as shoot, young leaves, flowers, fruits, and seeds (Gupta and Chakrabarty, 2013; Yano *et al*., 2015). In seeds, GA breaks seed dormancy and stimulates germination by increasing the growth potential of the embryo, through weakening of the seed cover and inducing gene expression involved in cell expansion (Gupta and Chakrabarty, 2013). In the aleurone layer of seeds, GA also induces hydrolytic enzymes involved in catabolism of nutrients used by the growing embryo. Although the GA response pathway is not fully understood, some components of the pathway have been uncovered. The GA response involves activity of GA receptors (gibberellin insensitive dwarf1, **GD1**, which localizes in the nucleus), the GA signaling repressor proteins **DELLA** (such as SLR1), and an **F-box protein** for DELLA degradation. In the absence of GA, SLR1 suppresses downstream activity of the pathway by suppressing the transcription factor GAMYB. When GA is present, it binds its receptor, and this interaction triggers SLR1 degradation, which allows for activation of GAMYB (Yano *et al*., 2015). The activation of GAMYB stimulates the expression of *Amy32b,* which encodes the hydrolytic enzyme α-amylase, and this mobilizes the endosperm reserves to feed the growing embryo (Gubler *et al*., 1995; Finkelstein *et al*., 2002).

Various observations in plants have supported the critical role of ABA and GA in regulation of seed germination and dormancy. In tomato and *Arabidopsis*, ABA-deficient and ABA-insensitive mutants show no dormancy, and in maize, the ABA-deficient mutant kernels precociously germinate on the ear during kernel development (White *et al*., 2000). This suggests that a threshold level of ABA is required to promote dormancy and prevent pre-harvest sprouting. GA is known to release seed dormancy, and incubating seeds in exogenous GA was shown to significantly increase germination and seedling height, and accelerated α-amylase activity. Seeds treated with GA showed increased degradation of starch and protein storage vacuoles, while this was diminished in the presence of ABA (Yu *et al*., 2016).

These observations suggest that pre-harvest sprouting could be caused by insufficient ABA or ABA insensitivity, or an upregulation of GA pathways. Although the mechanism is not fully understood, it is currently known that ABA antagonizes GA effects at the level of gene expression. It has been proposed that ABA can antagonize the GA-induced pathway through downregulation of GAMYB (Gomez-Cadenas *et al*., 2001), and there is some evidence to support this. The SnRK2 kinase that responds to ABA in wheat was identified to be PKABA1, and its mRNA levels increase rapidly in response to dehydration in seeds (Holappa and Walker-Simmons, 1995). PKABA1 has been shown to act as an intermediate in the ABA antagonism of GA-induced gene expression, because it was able to fully substitute for ABA in inhibiting the expression of α-amylase in GA-treated barley aleurone layers (Gomez-Cadenas *et a*l., 2001). Previously, our lab has shown that the wheat (*Triticum aestivum*) transcription factor TaABF1, a member of the ABF family of bZIP factors, interacts with PKABA1, and PKABA1 was able to phosphorylate synthetic TaABF1 peptides (Johnson *et al*., 2002).

TaABF1 is an ABRE-binding transcription factor with the three conserved N-terminal sequence blocks that are distinctive for ABF proteins, as well as a bZIP domain that is highly

conserved with other members of the ABF family (Fig. 2) (Johnson *et al*., 2002). In addition to interacting with PKABA1, TaABF1 expression was found to be correlated with levels of seed dormancy and ABA sensitivity in wheat cultivars (Rikiishi *et al*., 2010). Additionally, constitutive expression of TaABF1 eliminated GA-induced expression from the *Amy32b* promoter and strongly stimulated expression from the ABA- inducible *HVA1* and *HVA22* promoters in aleurone cells of imbibing grains (Johnson *et al*., 2008)

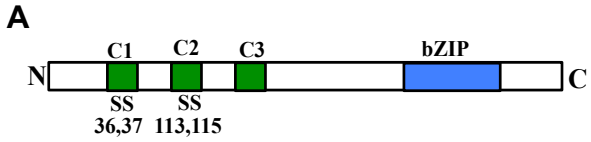

B

1 MASEMSKDVKFSEEEVTSHPRVLEGEEQAVAPARQSSIFALTLDELQYSV
51 CEAGRNFGSMNMDEFMSNIWNADEFQAATGGGLVGMEVAPVVGAGGGGGG
101 LDAGGSNLARQESFSLPPPLCRKTVDEVWAEINREPRPVHAQPQAARPSQ
151 QPPVQPSVPANDRQGTLGELTLEQFLVKAGVVRGSGAGGQAPVPVGMVHG
201 QMNPAQQGQQPGPMMYPIAPANGMFPAMGDGMGFIPNGYAGMVVVPPPPP
251 PQGGVVGIVSPGSSDGRSAMTQADMMNCMGEGAMMENGGTRKRGAPEDQS
301 CERSIERRHRRMIKNRESAARSRARKQAYTVELEAELNHLKEENARLKAE
351 EKTILLTKKQMLVEKMIEQSKENVNAKKGAPLSRHCGSCIW

Figure 2. (A) Schematic of the wheat transcription factor TaABF1, indicating the three conserved regions and the bZIP DNA binding domain. S36, S37, S113, and S115 are phosphorylatable serine residues with a potential to regulate TaABF1 activity. (B) The amino acid sequence of TaABF1 with C1 (blue), C2 (green), C3 (red) highlighted. The DNA binding region is underlined.

These results suggest that TaABF1 is involved in the ABA pathway, where it promotes seed dormancy and inhibits seed germination by downregulating GA-induced genes (Fig. 3). The TaABF1's downregulating effect on *Amy32b* promoter was shown to be stronger in the presence of exogenous ABA, but western blot analyses showed that levels of TaABF1 were not significantly affected by the presence of exogenous ABA or GA. Analysis by isoelectric focusing gel showed a shift of TaABF1 to higher isoelectric point (pI) after phosphatase treatment (Harris *et al*., 2013), indicating that TaABF1 is phosphorylated *in vivo*. This suggests that changes in TaABF1

expression levels are not what regulates its role in ABA and GA responses, but rather phosphorylation patterns of TaABF1 could regulate its activity.

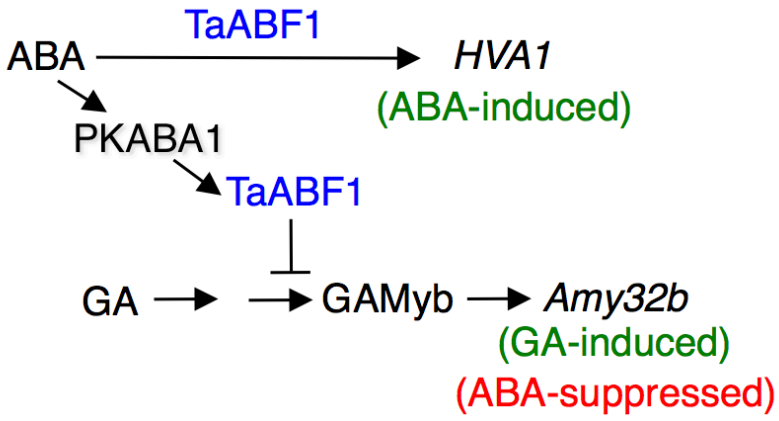

Figure 3. Diagram depicting the role of TaABF1 in upregulation ABA-induced genes and downregulation of ABA-suppressed genes.

In order to understand the role of TaABF1 in ABA and GA pathways, it is important to determine how phosphorylation regulates its activity. Since ABF transcription factors have regions that are conserved, it is predicted that their function as transcription factors is maintained in these regions. The TaABF1 amino acid sequence deduced from TaABF1 cDNA clones identified phosphorylatable residues in the conserved regions C1 and C2 (Fig. 2) (Johnson *et al.*, 2002). Using site-directed mutagenesis, these residues can be mutated to alanine (not phosphorylatable) or aspartate (phosphomimetic) and be used to study the basis of phosphorylation and how it affects activity in TaABF1. It is common in protein phosphoregulation studies to mutate phosphorylation sites to "phosphomimetic" residues, which introduces a negative charge and mimics a constitutively phosphorylated state. This approach was previously used by our group to analyze four serine residues S36, S37 (in C1), S113, and S115 (in C2) and how their phosphorylation status affect TaABF1 activity. Previous results indicated that altering all four sites to aspartate (S36D/S37D/S113D/S115D TaABF1 mutant) increased the ability of TaABF1 to upregulate the

ABA-induced *HVA1* and downregulate the ABA-repressed *Amy32b* promoters (Johnson *et al*., 2015). With the four residues mutated to alanine (S36A/S37A/S113A/S115A TaABF1 mutant), TaABF1 activity was indistinguishable from wild type. S36D/S37D and S113D/S115D mutants were more active than their wild type counterpart, but less active than the 4xD mutant. In contrast, S113D mutant TaABF1 was found to have reduced TaABF1 activity, indicated by inability to upregulate *HVA1* and downregulate *Amy32b* promoters. This indicates that phosphorylation of these serine residues affects TaABF1 activity and suggests that these residues might thus be the regulatory sites of the transcription factor.

The new work reported in this thesis aims to explain the role of TaABF1 in ABA and GA pathways by further characterizing the role of phosphorylation of individual serine residues in TaABF1 regulation, determining the sites of TaABF1 phosphorylation *in vivo*, and assessing how ABA and GA hormones affect these phosphorylation patterns. Since the S113D mutation reduced TaABF1 activity, we hypothesized that a S36D/S37D/S115D TaABF1 mutant might be more active than the S36D/S37D/S113D/S115D TaABF1 mutant. We tested this by preparing TaABF1 effector constructs with the three altered serine residues; S36D/S37D/S115D and S36A/S37A/S115A, and assessed their ability to upregulate *HVA1* and downregulate *Amy32b* promoters in barley aleurone layer using particle bombardment. As a complement to this work, we also attempted to identify TaABF1 phosphorylation sites in untreated wheat grains by exposing purified TaABF1 to aleurone kinases and analyzing the resulting phosphorylation patterns using tandem mass spectrometry.

Materials and Methods

For a detailed list of materials and purchase information, see supplemental table of materials, adapted from Uwase *et al*. 2018.

Bombardment

Methods for preparing gene constructs have been previously described: pAHC18 UBI::*LUCIFERASE* internal control plasmid (Christensen and Quail, 1996), *Amy32b::GUS* reporter construct (Lanahan *et al*., 1992), and *HVA1::GUS* reporter construct (Shen *et al*., 1993). The *UBI::TaABF1* effector constructs (Johnson *et al*., 2008). TaABF1 serine residues were mutated as described in Allison Smith's thesis (Smith, 2014).

Embryos from Himalaya barley seeds (a gift from the Department of Crop and Soil Sciences, Washington State University) were removed, and the embryoless seeds were sterilized with 10% household bleach and sterile water, and were imbibed for 48 hr. Seed coats were removed from the seeds to expose aleurone cells and the peeled seeds were incubated with or without 1 μM GA at 24ºC for 24 hr. The peeled seeds were bombarded with appropriate gene constructs following the established particle bombardment protocol (Uwase *et al*., 2018).

Seed Grinding

After particle bombardment, the seeds were incubated at 24ºC for 24 hr. Seed grinding was done using a Qiagen TissueLyser. A 5-mm stainless steel bead from Qiagen was added in 2.0 mL tubes and 800 μL of grinding buffer was added. Four embryoless seeds were blotted dry and added in each tube, and the tubes were placed in prechilled TissueLyser blocks. The blocks were mounted on the Quiagen TissueLyser and were shook at 30 Hz for 3 min. The blocks were then chilled on ice for 5 min and remounted after rotating racks in the opposite orientation, and the seeds were shaken

again at 30 Hz for 3 min. Both steps were repeated once more (for a total of 2 x 3 min shake on each side, with 5 min chilling on ice after each shake). The tubes with seed extracts were centrifuged at 4ºC for 10 min, and the supernatant was stored on ice until ready for luciferase and GUS assays. Luciferase and GUS assays were performed as previously described (Harris *et al*., 2013; Smith, 2014).

Determining TaABF1 phosphorylation sites

i. Purification of TaABF1 from E. coli

$(His)_6$-tagged TaABF1 on a p17 plasmid was expressed in *E. coli* (BL21(DE3)pLysE) cells. Cells were cultured in LB broth containing 100 μg/mL ampicillin and 34 μg/mL chloramphenicol. Expression was induced with 1 mM IPTG. TaABF1-expresssing *E. coli* cells were harvested by centrifugation at 6000 x g for 10 min at 4°C and stored at -80°C.

TaABF1 purification was done using the ProBond Purification System (from ThermoFisher) under denaturing conditions. The bacterial cell lysate was prepared by resuspending the cell pellets in Native Purification Buffer (250 mM monobasic sodium phosphate, 2.5 M NaCl, pH 8.0), sonicating on ice for 3 x 15 s, and centrifuging at 8000 x *g*, 4°C for 8 min. The supernatant was discarded, and the cell pellet containing tagged TaABF1 was resuspended in Guanidinium Lysis Buffer (6 M guanidine hydrochloride, 20 mM sodium phosphate, 500 mM NaCl, pH 7.8). The cell suspension was mixed at room temperature for 10 min, incubated on ice for 5 min, and sonicated again for 3 x 15 s pulses. The suspension was stored on ice for 5 min and centrifuged at 3000 x g, 4°C for 15 min.

Purification was done using the ProBond nickel column in denaturing conditions. The column was prepared per manufacturer's instructions, and $(His)_6$ ::TaABF1 was bound on the column for 30 min with shaking at room temperature. The purified TaABF1 was transferred to

native conditions (20 mM Tris pH 7.4 100 mM NaCl) and concentrated using spin filtration with 4 mL 10,000 MWCO centrifugal filter tubes.

ii. Preparation of aleurone extracts and phosphorylation assay

Embryos from NuWest wheat seeds (a gift from the Department of Plant Sciences and Plant Pathology, Montana State University) were removed, the seeds were sterilized with 10% bleach and sterile water, and were imbibed for 96 hr. Aleurone cells were isolated by splitting the embryoless wheat seeds in half and gently scraping the starch to leave the aleurone layer and seed coat. The seed coats with aleurone cells were ground using a mortar and pestle in 1.6 mL grinding buffer (1 mM DTT, 0.1% PVPP, 1 mM PMSF, 1% protease inhibitor, 1% phosphatase inhibitors, 50 mM Tris pH7.6). The seed suspension was centrifuged twice at 10,000 rpm, 4°C for 15 min and the supernatant was stored on ice until needed.

The phosphorylation assay was performed by incubating 1000 µL aleurone extract with 400 µg of the purified His-TaABF1 in Tris buffer (1% protease inhibitor, 1% phosphatase inhibitors, 20 mM Tris pH7.4) at 30° C for 60 min. TaABF1 was re-purified using the ProBond nickel column in denaturing conditions according to manufacturer's instructions.

iii. Trypsin digestion, phosphopeptide enrichment, and LC-MS/MS analysis

The re-purified TaABF1 was run on an SDS-PAGE gel, stained with Coomassie blue dye and destained in deionized water overnight. The TaABF1 band at 45 kDa was excised and cut into 1 mm square pieces. The In-Gel Tryptic Digestion Kit from ThermoFisher was used to digest protein samples according to manufacturer's manual. Digestion was done at 30°C overnight. The digested samples were mixed with 50% acetonitrile and incubated for 5 min at room temperature and dried in a speed vacuum.

Phosphopeptide enrichment was done on a TiO_2/ZrO_2 surface (TopTip TT2TiZr.96 from Glygen Corporation). Tips were washed 3x with 150 µL loading buffer (2% formic acid/ 50% acetonitrile). Dry peptides were resuspended in 150 µL loading buffer and these samples were added to the tips and washed 3x with 150 µL loading buffer. Elution was done with 50 µL elution buffer (1.5% NH_4OH/50% acetonitrile, pH 10.60). Elution was done for 4x and peptides were dried at room temperature in a speed vacuum

Orbitrap LC-MS/MS was run at the University of Rochester Proteomics Center and analyzed using MaxQuant Software for Proteomics (version 1.6.0.1) with Andromeda search engine.

iv. Analyzing results with MaxQuant

Results were received in .RAW file format and were analyzed following instructions detailed by Tyanova *et al* (Tyanova *et al*., 2016). Analysis was run against *Triticum aestivum* and *E. coli* proteomes from Uniprot (Uniprot IDs; AUP000019116_4565 and AUP000000625_83333 respectively). Following are settings that were changed from default:

- Group-specific parameters: Type = Standard, Multiplicity =1; Digestion = trypsin, missed cleavages = 2; variable modifications: Oxidation (M), Acetyl (protein N-term), phospho (STY); Instrument type = Orbitrap.
- Global parameters: Fixed modifications = carbamidomethyl (C), Minimum peptide length = 4; Identifications: FDR PSM = 0.01, Protein FDR= 0.01, Site decoy = 0.01, Minimum peptides = *2,* Minimum unique peptide = *1*.
- Number of threads ≥ 10

The data were visualized using details from Tyanova *et al* (Tyanova *et al*., 2015) and analyzed using R, the software environment for statistical computing and graphics (version 3.4.3).

Results

Phosphomimetic TaABF1 mutants show increased activity in downregulating *Amy32b* promoter

Evidence shows that the *Amy32b* promoter is activated by GA and inhibited by ABA or high levels of TaABF1. Previous work indicated that simultaneous mutation of TaABF1 phosphorylatable serine residues S36, S37, S113, and S115 to phosphomimetic aspartate (4xD) increased TaABF1 ability to downregulate the *Amy32b* promoter. Since a S113D TaABF1 mutant was less active compared to its wildtype counterpart, we tested whether a S36D/S37D/S115D mutant would have even more activity than the 4xD mutant. TaABF1 mutants S36D/S37D/S115D and S36A/S37A/S115A on ubiquitin promoters were successfully introduced in aleurone cells of barley grains via particle bombardment. TaABF1 activity was measured using the GUS reporter system (Fig. 3A). As expected, there was very little detected GUS activity in the absence of GA hormone, and the GUS activity increased about 40 fold upon the addition of 1 μM GA, which emphasizes the role of GA in simulating expression from the *Amy32b* promoter. Similar to the 4xD TaABF1 mutant, the expression of reporter construct *Amy32b::GUS* in aleurone cells was inhibited in the presence of *UBI:: (S36D/S37D/S115D) TaABF1* effector compared to the wild type TaABF1 (Fig. 3B). At low dose of wild type and mutant TaABF1 transgenes, there was no observable difference of normalized GUS activity between seeds that were exposed to wild type, 3xA, and 3xD TaABF1. At high dosage, the 3xD TaABF1 mutant caused a decrease in the normalized GUS activity to about half the activity observed with wild type TaABF1, but the 3xA mutant did not show a difference in GUS activity compared to its wild type TaABF1 counterpart. These results indicate that the 3xD TaABF mutant does not have higher activity than the 4xD TaABF1 mutant in downregulating the *Amy32b* promoter.

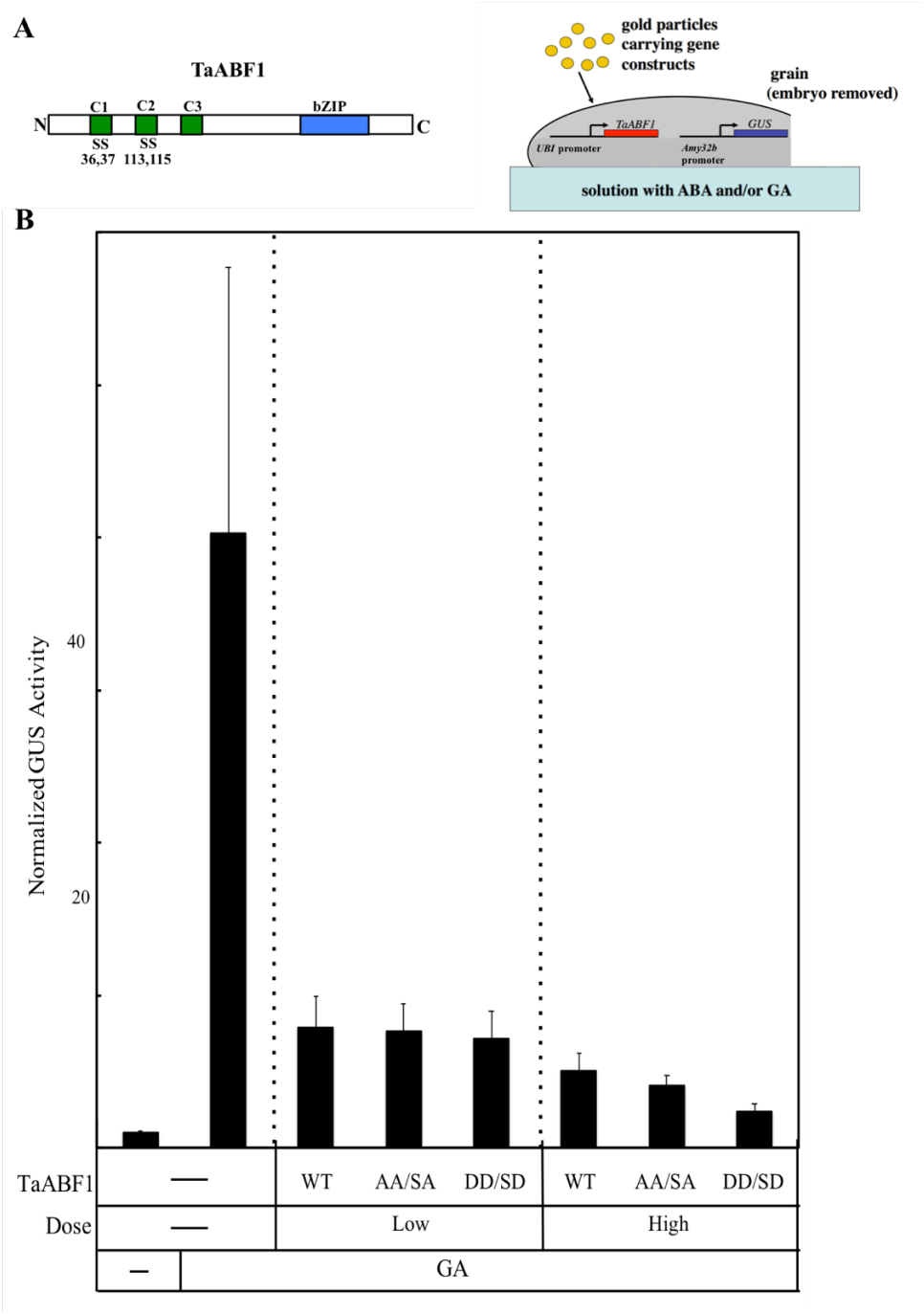

Figure 3. Phosphorylation of transcription factor TaABF1 increases its activity. (A)left; The transcription factor TaABF1 with conserved regions and potential phosphorylation sites highlighted. Right; schematic overview of particle bombardment protocol, highlighting gene constructs. (B) The effect of triple S36, S37, S115 mutations on TaABF1 activity. The reporter construct *Amy32b::GUS* was bombarded into barley aleurone cells with or without (-) the effector constructs *UBI::(S36A/S37A/S115A) TaABF1* or *UBI:: (S36D/S37D/S115D) TaABF1*, and the constructs were either introduced at low or high dose. GUS activity was normalized and bars indicate GUS activities ± SE after 24 h of incubation

The work up to this point has established that phosphorylation at specific serine residues on TaABF1 can strongly regulate its activity as a transcription factor. To complement that work, it is important to determine which residues on TABF1 are actually phosphorylated by protein kinases in aleurone cells, as well as the conditions that affect their phosphorylation patterns. To address this question, we mixed purified TABF1 with protein extracts from aleurone cells, and then looked for the presence of phosphorylation using mass spectrometry.

Detection of TaABF1 peptides by LC-MS/MS

Recombinant $(His)_6$ TaABF1 was purified from *E. coli* cell pellets using the ProBond nickel column under denaturing conditions, and then transferred to native conditions. A thick band was observed around 45 kDa on an SDS PAGE gel (Fig. 4), corresponding to the size of His-tagged TaABF1. Measuring the protein concentration using the Bradford assay indicated a yield of 500-800 μg from 50 mL of cell culture.

Aleurone layers were isolated from wheat grains and ground into an extract containing kinases. The extract was incubated with approximately 500 μg of the purified recombinant His-tagged TaABF1. TaBF1 was then re-purified using a nickel column under denaturing conditions, a yield of 380 μg was obtained, and a thick band of 45 kDa was observed (Fig. 4). The re-purified TaABF1 band was cut out of the gel and was digested with trypsin, analyzed using LC-MS/MS, and results were analyzed using MaxQuant Software for Proteomics (version 1.6.0.1) with Andromeda search engine. In the second trial, phosphopeptides were enriched on a TiO2/ZrO2 column, and analyzed using LC-MS/MS.

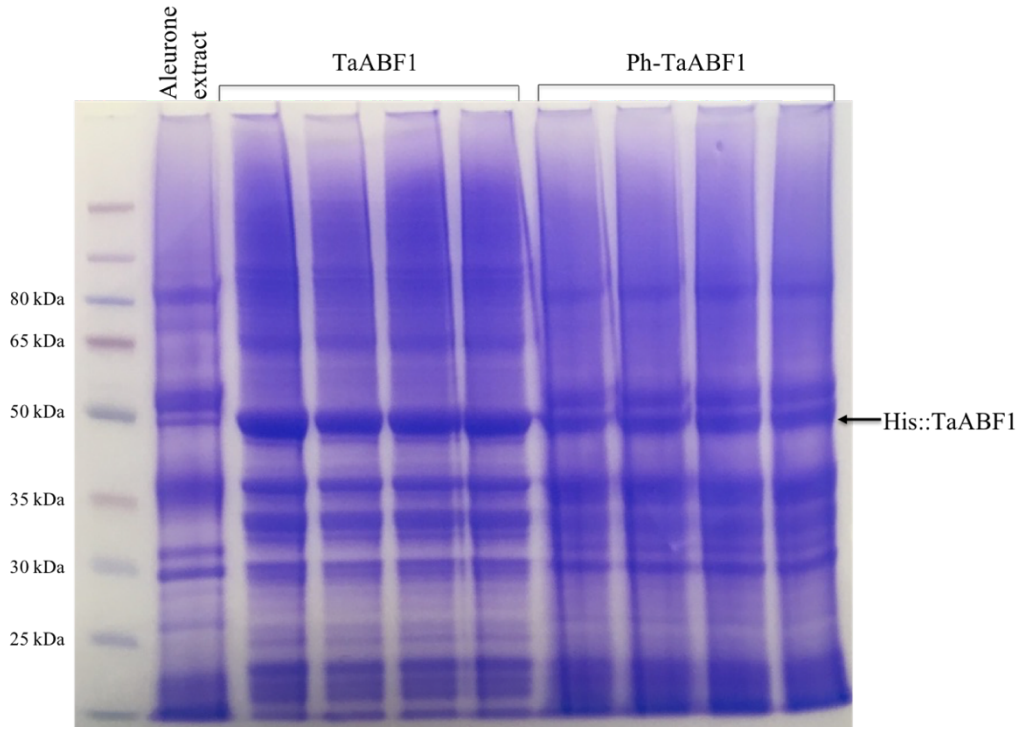

Figure 4. TaABF1 was purified from *E. coli* cells under denaturing conditions and separated on as SDS gel (TaABF1 lanes, 32 μg per lane). The purified TaABF1 was incubated with aleurone kinases, re-purified under denaturing conditions, and separated on an SDS gel (Ph-TaABF1 lanes, 47 μg per lane). Lane 2 is the aleurone extract with no TaABF1. The gel was stained with Coomassie Blue Dye.

TaABF1 samples were divided in two categories, one that was not treated with aleurone kinases (untreated TaABF1), and one that was treated with aleurone kinases and re-purified before LC-MS/MS analysis. The experiment was done in two trials, where trial one (T1) aleurone kinase treatment was done by incubating TaABF1 with aleurone kinases for 1 hr, and in trial two (T2), incubation was done for 4 hr, and phosphopeptides were enriched on a TiO_2/ZrO_2 surface prior to Orbitrap liquid chromatography mass spectrometry. The chromatograms of all samples indicated that there were differences in elution patterns across trials, with T2 samples having slightly higher intensities (fig. 5).

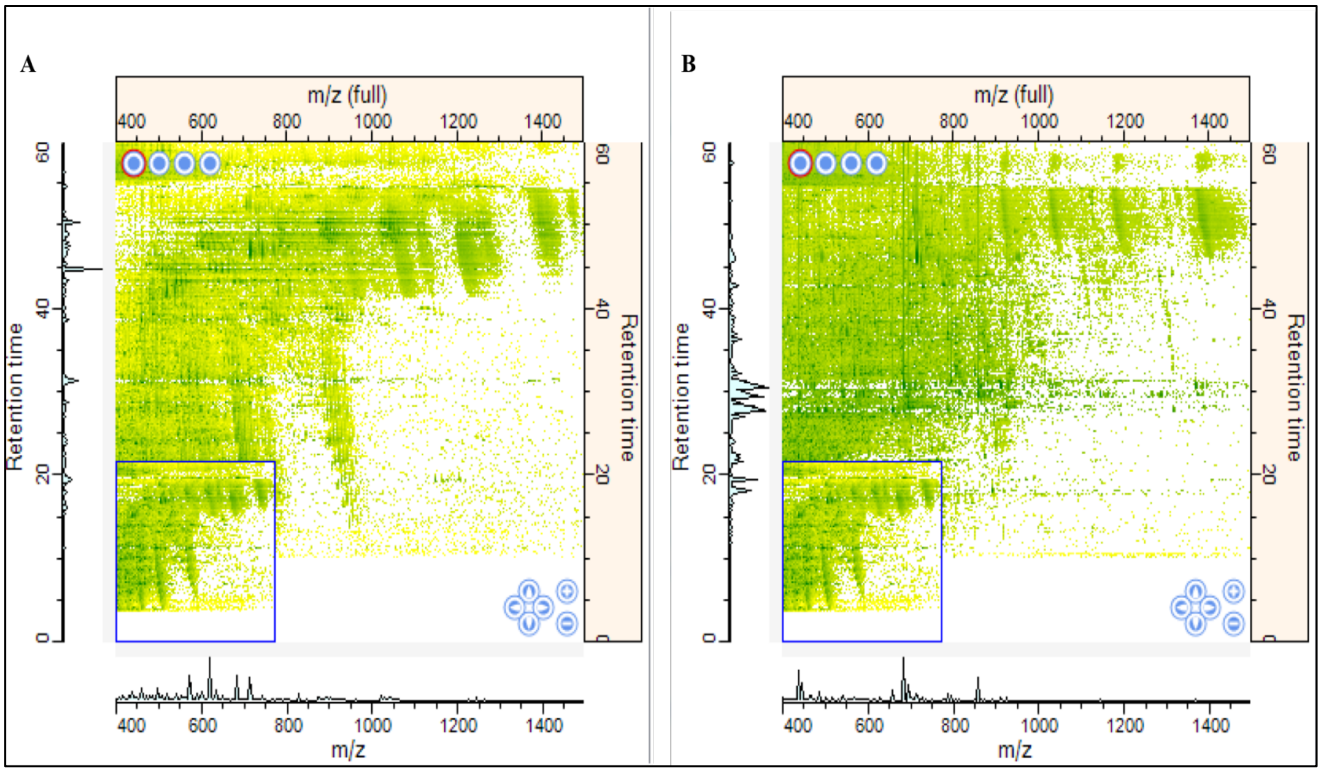

Figure 5. Chromatograms showing elution patterns of (A) untreated T1 sample and (B) untreated T2 sample. Retention time is in minutes.

For identification of individual proteins in each analyzed sample, proteins were scored as present if at least ten unique peptides were identified (note that MaxQuant counts peptides with missed cleavages as unique). Under the stated parameters, 12 proteins from wheat were identified, as well as 6 human contaminants. Four of the wheat proteins were previously uncharacterized. In both trials, there were more wheat protein contaminants in treated than untreated samples, but T2 samples had more contamination overall. In all samples, TaABF1 was by far the most abundant protein (Fig. 6). The 41.802 kDa TaABF1 was identified with a 55.5% sequence coverage, an intensity of 2.5×10^{11}, a score of 323.31, and a total of 1138 MS/MS counts. The protein score value is derived from peptide posterior error probabilities (p- value for peptide identification), and it validates the level of confidence for protein identification. High scores indicate high confidence for identification.

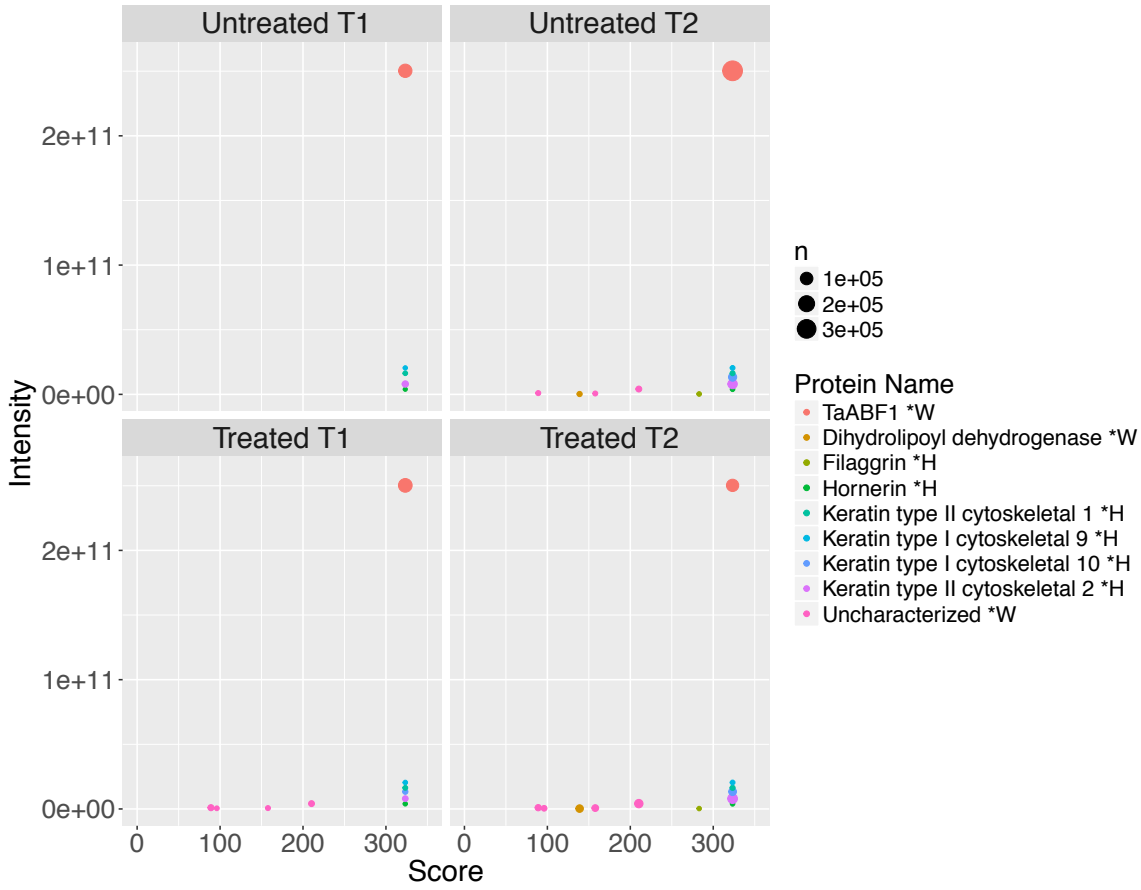

Figure 6. TaABF1 protein was identified at highest intensity and scores in all samples. The point size depends on the number of observations made per protein. *W and *H refer to wheat or human proteins respectively.

We found that the untreated samples contained more peptides overall, and T1 samples had more TaABF1 peptides than T2 samples (untreated T1: 44 peptides, treated T1: 44 peptides, untreated T2: 29 peptides, treated T2: 22 TaABF1 peptides). In all samples, 14 peptides with no missing cleavages were observed. However, most peptides had one to two missing cleavages, and these were not excluded from the analysis, since phosphorylation is independent of peptide cleavage, and removing the peptides with missing cleavage would lower the probability of finding phosphorylated peptides. Including those with missing cleavages, a total of 44 TaABF1 peptides were observed (Table 1). T2 samples had fewer TaABF1 peptides compared to T1 samples, but there was no noticeable difference in the number of TaBF1 peptides within trials. Most peptides

were observed with +1 to +4 charge, but a few had up to + 5 (only one had +6) (Fig. 7A). There was a positive correlation between charge and peptide mass, which is affected by the number of missed cleavages (figure not shown). There were no visible differences in the intensities of identified peptides between samples. Though T2 samples had fewer peptides, they had more MS/MS counts per peptide (Fig. 7B). Each peptide had multiple retention times as a function of charge and missed cleavages, but the retention times were consistent between samples (data not shown).

Table 1. TaABF1 peptides identified in all samples and their properties.

Pep code	Sequence	Missed cleavages	Charges	Mass (kDa)	Intensity	Score	P value
T-8	DVKFSEEEVTSHPR	1	2;3;4	1658.79	5.07E+09	343.65	4.20E-96
T-8	DVKFSEEEVTSHPRVLEGEEQAVAPAR	2	3;4;5	3008.48	3.45E+08	301	2.50E-79
T-11	FSEEEVTSHPR	0	1;2;3	1316.6	6.60E+10	287.48	3.70E-41
T-11	FSEEEVTSHPRVLEGEEQAVAPAR	1	3;4	2666.29	1.12E+08	395.87	7.10E-174
T-22	VLEGEEQAVAPAR	0	1;2;3	1367.7	3.91E+10	238.51	1.40E-46
T-22	VLEGEEQAVAPARQSSIFALTLDELQYSVCEAGR	1	3;4	3735.84	7.07E+08	252.96	3.90E-64
T-35	QSSIFALTLDELQYSVCEAGR	0	2;3	2386.15	1.52E+09	458.64	1.40E-239
T-111	QESFSLPPPLCR	0	1;2;3	1429.7	6.30E+09	258.52	7.60E-30
T-111	QESFSLPPPLCRK	1	2;3	1557.8	5.74E+08	254.24	6.30E-30
T-123	KTVDEVWAEINR	1	2;3	1458.75	4.50E+09	322.27	2.40E-79
T-123	KTVDEVWAEINREPRPVHAQPQAARPSQQPPVQPSVPANDR	2	4;5	4594.35	9.85E+07	200.04	3.90E-40
T-124	TVDEVWAEINR	0	2;3	1330.65	9.40E+08	253.64	3.20E-29
T-124	TVDEVWAEINREPRPVHAQPQAARPSQQPPVQPSVPANDR	1	4;5;6	4466.26	2.02E+08	187.45	2.30E-33
T-135	EPRPVHAQPQAARPSQQPPVQPSVPANDR	0	3;4;5	3153.62	9.01E+09	177.85	1.20E-20
T-164	QGTLGELTLEQFLVK	0	2;3	1674.92	2.30E+09	300.89	6.40E-23
T-268	SAMTQADMMNCMGEGAMMENGGTR	0	2;3	2579.97	0.00E+00	199.01	2.10E-43
T-268	SAMTQADMMNCMGEGAMMENGGTRK	1	3	2708.06	1.25E+06	95.82	2.60E-04
T-268	SAMTQADMMNCMGEGAMMENGGTRKR	2	4	2864.16	3.17E+06	152.07	3.50E-09
T-292	KRGAPEDQSCER	2	2;3	1431.65	1.94E+09	183.33	7.20E-06
T-293	RGAPEDQSCER	1	2;3	1303.56	6.21E+08	253.71	4.70E-29
T-293	RGAPEDQSCERSIER	2	3;4	1788.82	2.11E+07	244.05	1.30E-23
T-294	GAPEDQSCER	0	1;2	1147.46	1.74E+09	186.3	1.60E-08
T-294	GAPEDQSCERSIER	1	2;3	1632.72	1.05E+08	203.51	5.60E-06
T-294	GAPEDQSCERSIERR	2	2;3;4	1788.82	2.01E+08	125.53	4.70E-05
T-326	KQAYTVELEAELNHLKEENAR	2	2;3;4;5	2484.26	1.37E+10	434.7	2.70E-106
T-327	QAYTVELEAELNHLK	0	2;3	1756.9	1.40E+08	242.82	2.30E-23
T-327	QAYTVELEAELNHLKEENAR	1	2;3;4	2356.17	1.09E+10	653	0.00E+00
T-327	QAYTVELEAELNHLKEENARLK	2	5	2597.34	9.70E+06	157.97	5.00E-09
T-347	LKAEEK	1	1	716.41	3.77E+07	153.15	1.10E-02
T-347	LKAEEKTILLTK	2	2;3	1385.85	5.32E+08	266.93	5.80E-38
T-349	AEEKTILLTK	1	2	1144.67	0.00E+00	185.33	1.20E-15
T-349	AEEKTILLTKK	2	2;3	1272.77	4.08E+07	199.08	1.90E-04
T-353	TILLTKK	1	1;2	815.55	5.69E+08	142.64	2.60E-03
T-353	TILLTKKQMLVEK	2	3	1543.94	1.66E+07	121.76	6.40E-04
T-359	KQMLVEK	1	1;2	874.49	4.56E+10	178.08	1.90E-04
T-359	KQMLVEKMIEQSK	2	3	1590.85	5.42E+05	163.27	9.20E-05
T-360	QMLVEK	0	1	746.4	7.61E+06	121.29	5.70E-03
T-360	QMLVEKMIEQSK	1	3	1462.75	1.60E+07	108.72	2.00E-04
T-360	QMLVEKMIEQSKENVNAK	2	2;3;4	2118.08	7.01E+08	439.61	1.90E-117
T-366	MIEQSK	0	1	734.36	1.31E+09	105.39	1.50E-03
T-366	MIEQSKENVNAK	1	2;3	1389.69	3.36E+10	293.88	2.60E-21
T-366	MIEQSKENVNAKK	2	2;3	1517.79	3.29E+08	276.95	9.40E-21
T-372	ENVNAK	0	1	673.34	1.66E+06	172.39	3.20E-02
T-385	HCGSCIW	0	2	918.35	1.40E+09	112.58	2.60E-02

* Highlighted are S36 and S37 (in T-35) and S113 and S115 (in T-111)

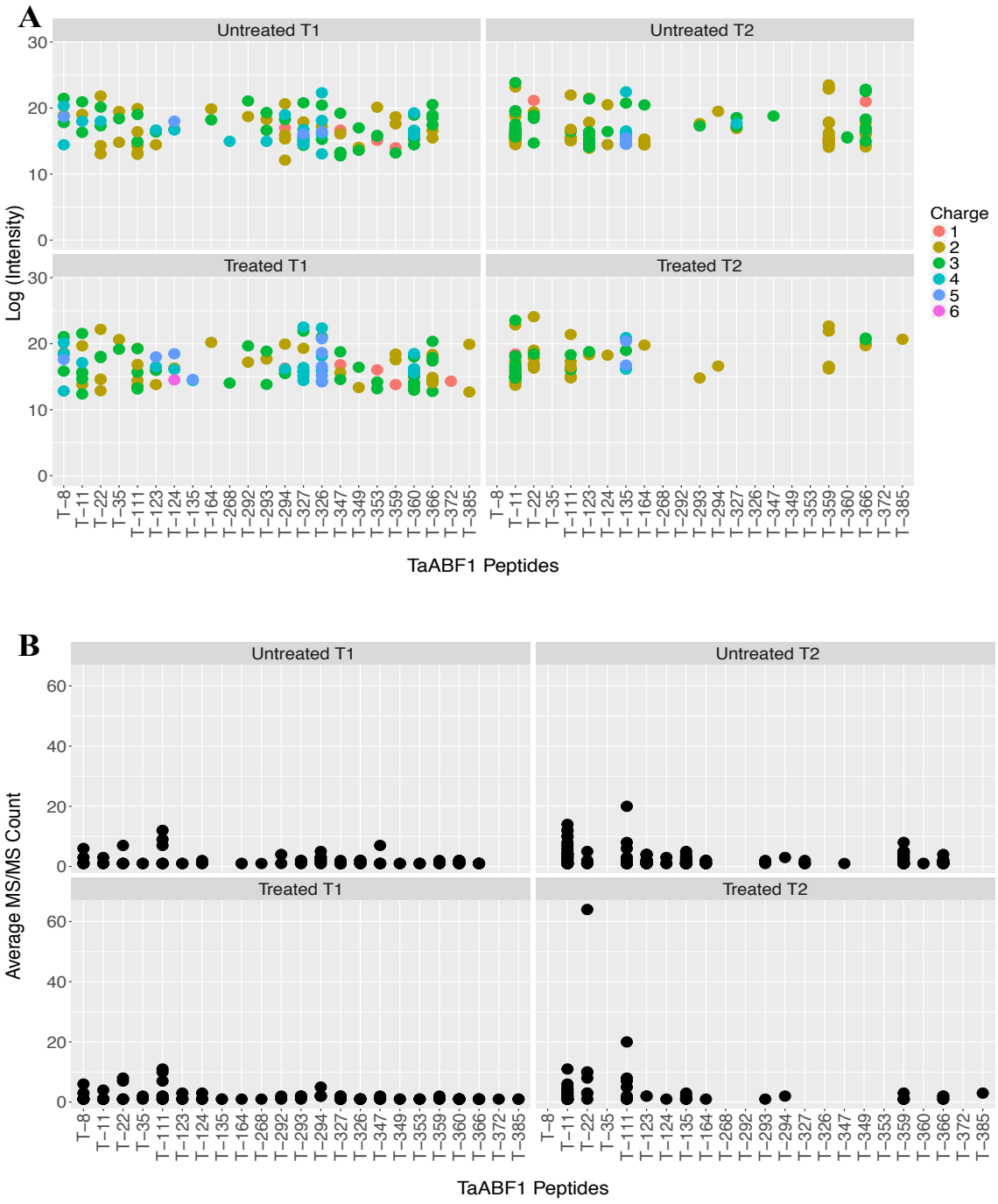

Figure 7. Identified TaABF1 peptides showing (A) their intensities and respective charges, and (B) their average MS/MS count. Each peptide had different forms depending on the number of missed cleavages, charge, and differences in retention time

Based on our previous work, we were interested in seeing if S36, S37, S113, and S115 would be phosphorylated by aleurone kinases. These are found on peptides T-35 (S36 and S37) and T-111(S113 and S115) that are in TaABF1 conserved regions C1 and C2 respectively. We also looked at phosphorylatable regions in C3 (T-164) and TaABF1's DNA binding region (T-317). T-35 was only seen in T1 samples, with both +2 and +3 charges. T-111 had most occurrences and was seen in all samples with +1, +2, and +3 charges. T-164 was also seen in all samples at +2 and +3 charges. T-317 was not found in any of the samples (Fig. 8A). The average retention time for each of these peptides was fairly consistent across samples, regardless of the number missed cleavages (Fig. 8B). An example of the clear identification of one particular peptide (T-35) by LC-MS/MS is shown in figure 9A and B. The chromatograms and MS/MS spectra of phosphorylatable peptides indicated that the peptides were detected at high resolution and intensities.

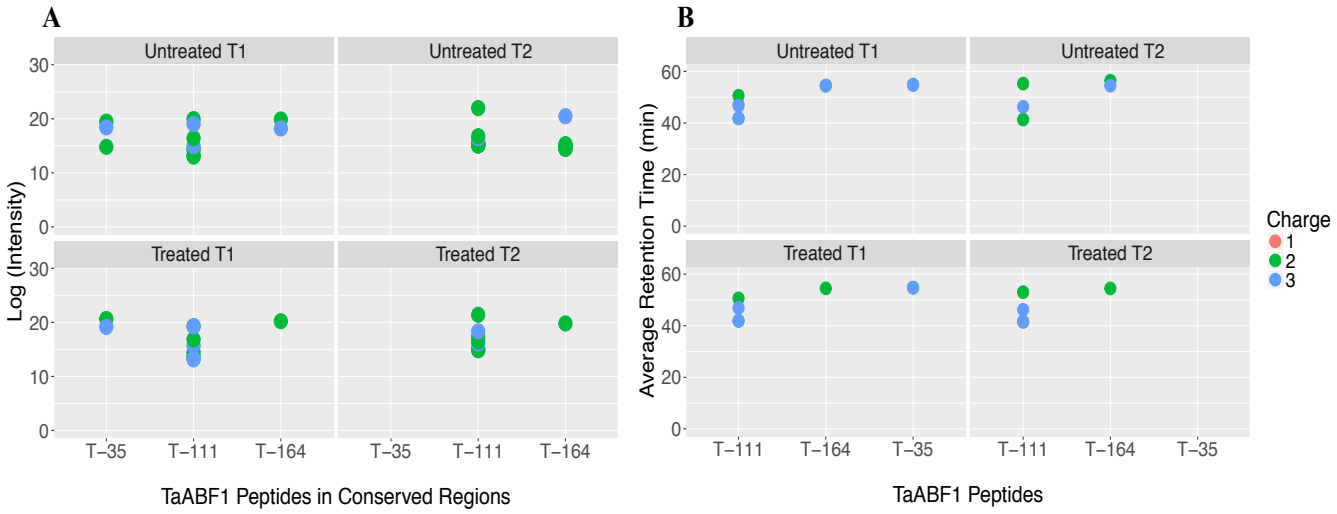

Figure 8. Identified TaABF1 peptides with phosphorylation potential, found in the protein's conserved region. Given are their intensities and charges found, as well as the average retention times

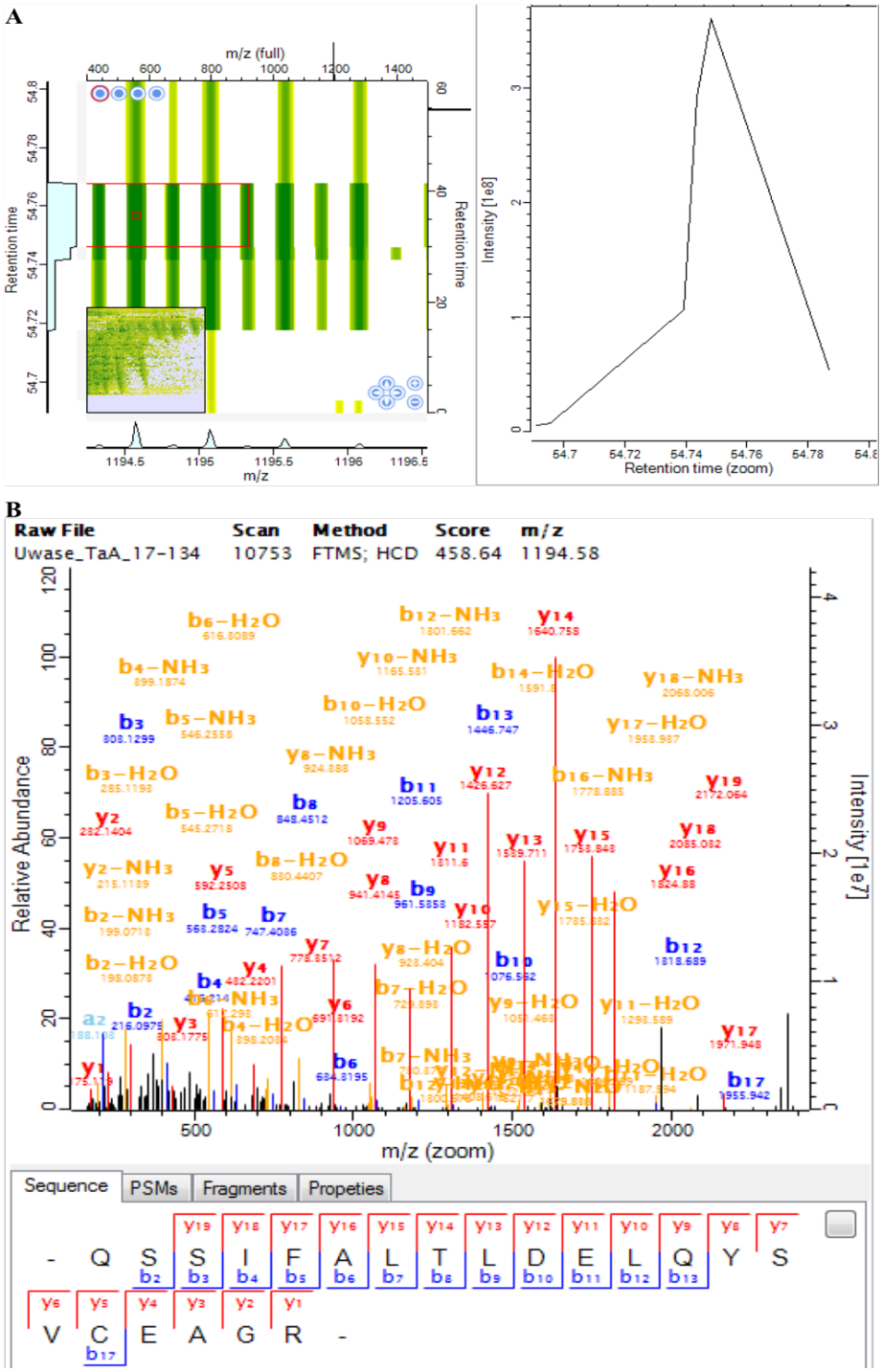

Figure 9. Clear identification of T-35 by LC-MS/MS. Shown is (A) the full and zoomed chromatograms, as well as (B) its corresponding MS/MS spectrum.

In vitro TaABF1 phosphorylation by wheat aleurone kinases was not detected

In tandem mass spectrometry, the masses of intact peptide ions are determined in MS1 and then the peptides are isolated and fragmented to ions that are detected in MS2. On MS/MS, phosphopeptides can be identified from 80 Da shifts due to their typical neutral loss of phosphoric acid upon fragmentation (McLachlin and Chait, 2001). MaxQuant is capable of determining the accurate phosphorylation site in a given peptide, and these results are compiled in a table along with phosphopetides' properties and their respective proteins. Unfortunately, we were not able to detect any phosphorylated TaABF1 peptides in any of the samples, since no mass shift was observed for any of the observed peptides (Fig. 10). To ensure that it was not a problem with MaxQuant's ability to detect phosphopeptides since we had clearly identified the phoshorylatable TaABF1 peptides, we looked for phosphorylation in all proteins and found 2 proteins with phosphorylation under default parameters. We also lowered the threshold of accepted scores of modified peptides (Min. score for modified peptides = 0 instead of default 40, and Min. delta score for modified peptides = 0 instead of default 6), and more phosphorylated peptides were detected, but none from TaABF1, indicating that failure of detection of phosphorylated TaABF1 peptides is not due to stringent parameters.

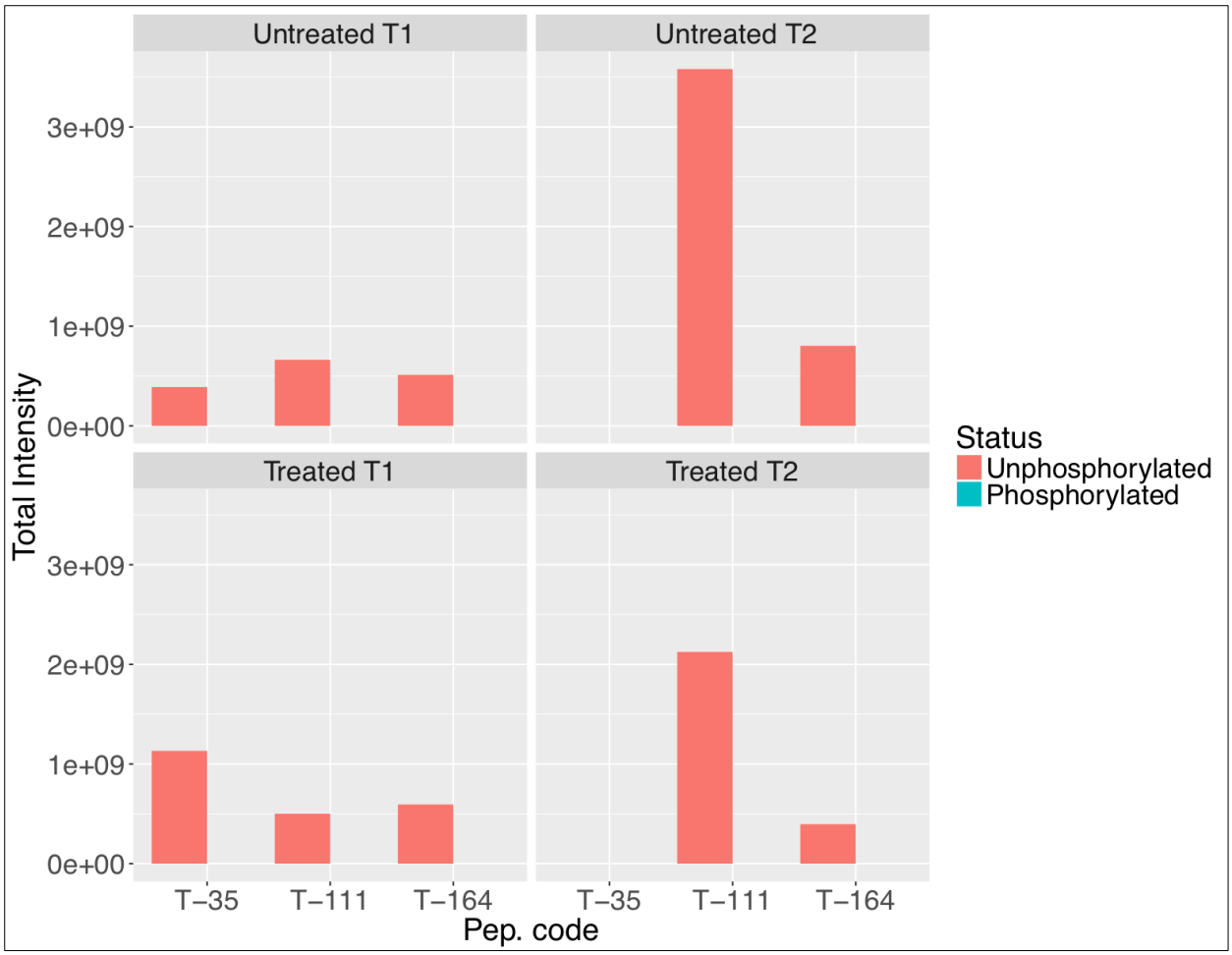

Figure 10. There was no observed TaABF1 phosphorylation under the given conditions. (B) Intensity of unphosphorylated and phosphorylated peptides in the conserved region. Total intensity is the sum of intensities for all observed forms of a given peptide.

Discussion

TaABF1 has been shown to be at the intersection of the GA and ABA pathways, where it upregulates the ABA-induced response and inhibits the GA-induced responses in regulating seed dormancy in cereal grains. However, its mechanism of action and regulation remains elusive. Harris *et al*, 2013 showed that the presence of ABA and GA hormones strongly affect TaABF1 activity, but the hormones do not affect TaABF1 protein levels. This implies that the TaABF1 role in enhancing ABA and inhibiting GA responses depends on post-translational modification. The activity of many ABF transcription factors is known to be regulated by phosphorylation, and the SnRK2 kinase PKBAl was shown to have an ability to phosphorylate synthetic TaABF1 peptides (Johnson *et al*., 2002), indicating that phosphorylation might have a role in regulating TaABF1 activity. However, there is still little understanding of which TaABF1 residues are responsible for this phosphorylation-dependent regulation *in vivo*, and the role that specific amino acid residues have on TaABF1 regulation have not been fully characterized.

Phosphorylation of four serine residues in TaABF1 conserved region; S36, S37, S113, and S115 has been shown to affect TaABF1 activity, but the residues do not have additive effects on TaABF1 activity in barley aleurone cells. S36D/S37D/S115D TaABF1 upregulates *HVA1* promoter and downregulates *Amy32b* promoter, but this induction was not significantly higher than 4×D TaBF1, despite the fact that phosphorylation of S113 alone downregulates TaABF1 activity. This suggests that TaABF1 activity is regulated by phosphorylation of specific serine residues, not necessarily the phosphorylation of all of the sites together. We previously saw that there is no significant difference between S113D/S115D and S113A/S115A TaABF1 activity, and S36D/S37D mutant was less active than the 4×D TaABF1 (Johnson *et al*., 2015). Though there might be some additive phosphorylation effects on TaABF1 activity, the data also support the idea that all the

serine residues do not have similar roles in TaABF1 regulation, as supported by the effect of S113 phosphorylation on TaABF1 activity.

The role of serine residues in TaABF1 regulation is further supported by two serine residues in its DNA binding region (S318 and S322). Past experiments have shown that mutations of these residues (either phosphorylation or dephosphorylation) downregulates transcription from *HVA1* promoter, but has no effect on *Amy32b* promoter, suggesting that TaABF1 affects *Amy32b* by other means that do not involve DNA binding, but also that individual serine residues have different tasks in TaABF1 regulation. The fact that S36A/S37A/S115A TaABF1 mutant functions similarly to wild type TaABF1 suggests that under the given bombardment conditions, in the presence of GA, the serine residues might be unphosphorylated, even though their phosphorylation would enhance TaABF1 activity. Since expression from the GA-induced *Amy32b* promoter is suppressed under stress conditions, these results suggest that TaABF1 is underactive in favorable conditions when seeds are germinating, and it gets turned on through phosphorylation in response to some stressful environmental changes to upregulate expression from *HVA1* promoter. Having established that phosphorylation of TaABF1 affects its activity as a transcription factor, it is important to know the conditions under which this phosphorylation occurs and how different residues are involved in the regulation of TaABF1 activity. We utilized mass spectrometry to explore this question.

In the experiments reported here, we were not able to detect phosphorylation of TaABF1 after incubation *in vitro* with aleurone extracts in the absence of GA and ABA. However, through isoelectric focusing analysis and phosphatase treatment, Harris et. al 2013 determined that TaABF1 in aleurone layers is phosphorylated in the presence or absence of GA hormone treatment. This suggests that our failure to detect TaABF1 phosphopeptides could be associated with experimental difficulties. For instance, it is possible that phosphorylation occurs at low levels that the peptides could not be detected under MS/MS. We attempted to enhance the probability of detecting

phosphorylated peptides using by phosphopeptide enrichment on a TiO_2/ZrO_2 surface (T2 experiment). However, there was no improvement in the detected TaABF1peptides. In fact, less TaABF1 peptides were detected since some get lost through enrichment washes. Phosphoenrichment experiments are known to improve the detection of phosphopeptides by binding the peptides onto a column via phosphate groups, allowing unphosphorylated peptides to be washed away. More experiments will need to be done in order to optimize our phosphoenrichment experiment, and we can also increase the overall protein concentration. The observation that there were more wheat contaminants in treated samples is consistent with the fact that it is incubated in wheat extracts, whereas untreated samples are purified from *E. coli*. T2 samples had overall more contamination, and this can be explained by the fact that there was a change in TaABF1 purification protocol, where a wash with denaturing wash buffer at pH = 5.3 was eliminated to increase the concentration of found TaABF1, but this also retained more contaminant proteins in the sample. Though some peptides were lost through the phosphoenrichment experiment, T2 samples showed to have more peptides overall, but this is because trypsin digestion was done on 8x more protein than T1 samples.

We were able to detect TaABF1 peptides in conserved regions; T-35 which contains S36 and S37, T-111 which contains S113 and S115 residues, as well as T-167 in C3 (but its residues were not tested in particle bombardment experiments). The conserved peptide residues were detected at high intensities, with high MS/MS counts, and with consistent retention times between samples. This indicates that we have a controlled and consistent way of detecting the peptides, thus increases confidence that phosphorylation can be detected if it occurs. Harris et. al. 2013 were able to confirm that (a) kinase(s) in aleurone cells is able to phosphorylate TaABF1, so it is unlikely that our failure to detect TaABF1 phosphorylation was due to the lack of kinases. However, more tests will need to be done to optimize conditions used in our *in vitro* assay to ensure that they are

appropriate for strong activity of aleurone kinases, such as pH, temperature, and incubation times. Another argument can be that TaABF1 does not fully gain its native confirmation after the initial purification from *E. coli*, thus does not get recognized by its kinase. However, previous experiments have shown that PKBA1 was able to phosphorylate synthetic TaABF1 peptides (Johnson *et al*., 2002), indicating that the kinase does not recognize the entire protein, rather the individual peptides. Therefore, TaABF1 conformation, as long as the phosphorylatable residues remain accessible to the kinase, should not affect its ability to get phosphorylated.

A current suggested mechanism for TaABF1 action is that in the ABA-mediated GA-inhibition, kinase PKBA1 activity triggers TaABF1 phosphorylation, which then suppresses transcription factor GAMYB to downregulate the *Amy32b* promoter and downregulate GA-induced responses. In the upregulation of BA-induced responses, it has been suggested that TaABF1 functions independent of PKBA1 to bind and activate the *HVA1* and *HVA22* promoters *(Johnson et al*., 2008), which means that TaABF1 might have another aleurone kinase, since TaABF1 phosphorylation also increases its activity in upregulating the *HVA1/HVA22* promoters. This mechanism is supported by our particle bombardment experiments, which suggest that phosphorylation of different TaABF1 residues may play a different role in regulating TaABF1 activity, so there could be different kinases for different TaABF1 residues. Since TaABF1 needs to be active at specific times during the plant's life to ensure proper development, we reason that it undergoes different hormone-induced phosphorylation patterns. This, as well as the current suggested mechanism, can be elucidated by determining phosphorylation patterns associated with different conditions, such as the presence of GA and/or ABA hormones. This will be tested by incubating the aleurone cells with ABA and/or GA hormones prior to phosphorylation assay, and LC-MS/MS offers a good and reliable tool to explore these phosphorylation patterns. Determining sites of TaABF1 phosphorylation under different conditions will give insights in what role specific

residues play in regulating TaABF1 activity, as well as the TaABF1 mechanism of action in regulating the ABA and GA pathways in imbibing cereal grains.

Acknowledgements

I would like to thank Russell Johnson for his guidance, support, and invaluable lessons throughout this project. I would also like to thank my labmates; Amanda Young, Jenna Laidley, and Omolara Akingba for their help in carrying out experiments, as well as previous members of the Johnson lab who foreshadowed this work. Thanks to my reader Kevin Rice, Judy Stone for advice on grain homogenization, and Lynn Hannum for advice on fluorometry.

References

Christensen AH, Quail PH (1996) Ubiquitin promoter-based vectors for high-level expression of selectable and/or screenable marker genes in monocotyledonous plants. Transgenic Res **5**: 213–218

Finkelstein RR, Gampala SSL, Rock CD (2002) Abscisic acid signaling in seeds and seedlings. Plant Cell **14**: 15–45

Gomez-Cadenas A, Zentella R, Walker-Simmons MK, Ho T-HD (2001) Gibberellin/abscisic acid antagonism in barley aleurone cells: site of action of the protein kinase PKABA1 in relation to gibberellin signaling molecules. Plant Cell **13**: 667–679

Gubler F, Kalla R, Roberts JK, Jacobsen J V (1995) Gibberellin-regulated expression of a myb gene in barley aleurone cells: evidence for Myb transactivation of a high-pI alpha-amylase gene promoter. Plant Cell **7**: 1879–1891

Gupta R, Chakrabarty SK (2013) Gibberellic acid in plant: still a mystery unresolved. Plant Signal Behav **8**: e25501-4

Harris LJ, Martinez SA, Keyser BR, Dyer WE, Johnson RR (2013) Functional analysis of TaABF1 during abscisic acid and gibberellin signalling in aleurone cells of cereal grains. Seed Sci Res **23**: 89–98

Holappa L, Walker-Simmons M. (1995) The wheat abscisic acid-responsive protein kinase mRNA, PKABA1, is up-regulated by dehydration, cold temperature, and osmotic stress. Plant Physiol **108**: 1208–1210

Johnson R, Yang X, Lutian J, Jay L, Butler G, Uwase G, Chelimo D, Lopez J (2015) Phosphorylation of the transcription factor TaABF1 during gibberellin and abscisic acid signaling in cereal grains. Am. Soc. Plant Biol. Annu. Meet.

Johnson RR, Shin M, Shen JQ (2008) The wheat PKABA1-interacting factor TaABF1 mediates both abscisic acid-suppressed and abscisic acid-induced gene expression in bombarded aleurone cells. Plant Mol Biol **68**: 93–103

Johnson RR, Wagner RL, Verhey SD, Walker-Simmons MK (2002) The abscisic acid-responsive kinase PKABA1 interacts with a seed-specific Abscisic acid response element-Binding Factor, TaABF, and phosphorylates TaABF peptide sequences. PLANT Physiol **130**: 837–846

Lanahan MB, Ho T-HD, Rogers SW, Rogers JC (1992) A gibberellin response complex in cereal a-amylase gene promoters. Plant Cell **4**: 203–21

McLachlin DT, Chait BT (2001) Analysis of phosphorylated proteins and peptides by mass spectrometry. Curr Opin Chem Biol **5**: 591–602

Miyakawa T, Fujita Y, Yamaguchi-Shinozaki K, Tanakura M (2013) Structure and function of abscisic acid receptors. Trends Plant Sci **18**: 259–266

Ohkuma K, Lyon JL, Addicott FT, Smith OE (1963) Abscisin II, an abscission-accelerating substance from young cotton fruit. Science (80-) **142**: 1592–1593

Rikiishi K, Matsuura T, Maekawa M (2010) TaABF1, ABA response element Binding Factor 1, is related to seed dormancy and ABA sensitivity in wheat (Triticum aestivum L.) seeds. J Cereal Sci **52**: 236–238

Rodríguez-Gacio M del C, Matilla-Vázquez MA, Matilla AJ (2009) Seed dormancy and ABA signaling. Plant Signal Behav **4**: 1035–1048

Sah SK, Reddy KR, Li J (2016) Abscisic acid and abiotic stress tolerance in crop plants. Front Plant Sci **7**: 571

Shen Q, Uknes SJ, Ho T-HD (1993) Hormone response complex in a novel abscisic acid and cycloheximide-inducible barley gene. J Biol Chem **268**: 23652–23660

Smith AE (2014) The effect of phosphorylation on transcription factor TaABF1 ' s ability to downregulate the Amy32b gene in cereal aleurone. Colby College

Tyanova S, Temu T, Carlson A, Sinitcyn P, Mann M, Cox J (2015) Visualization of LC-MS/MS proteomics data in MaxQuant. Proteomics **15**: 1453–1456

Tyanova S, Temu T, Cox J (2016) The MaxQuant computational platform for mass spectrometry–based shotgun proteomics. Nat Protoc **11**: 2301–2319

Uwase G, Enrico TP, Chelimo DS, Keyser BR, Johnson RR (2018) Measuring gene expression in bombarded barley aleurone layers with increased throughput. JoVE e56728

Wang M, Heimovaara-Dijkstra S, Duijn B Van (1995) Modulation of germination of embryos isolated from dormant and nondormant barley grains by manipulation of endogenous abscisic acid. Source: Planta **195**: 586–592

White CN, Proebsting WM, Hedden P, Rivin CJ (2000) Gibberellins and seed development in maize. I. Evidence that gibberellin/abscisic acid balance governs germination versus maturation pathways. Plant Physiol **122**: 1081–1088

Yano K, Aya K, Hirano K, Ordonio RL, Ueguchi-Tanaka M, Matsuoka M (2015) Comprehensive gene expression analysis of rice aleurone cells: probing the existence of an alternative gibberellin receptor. Plant Physiol **167**: 531–544

Yoshida T, Fujita Y, Maruyama K, Mogami J, Todaka D, Shinozaki K, Yamaguchi-Shinozaki K (2015) Four Arabidopsis AREB/ABF transcription factors function predominantly in gene expression downstream of SnRK2 kinases in abscisic acid signalling in response to osmotic stress. Plant, Cell Environ **38**: 35–49

Yu H, Wang L, Chen X, Yang Y (2016) Effects of exogenous gibberellic acid and abscisic acid on germination, amylases, and endosperm structure of germinating wheat seeds. Seed Sci Technol **44**: 64–76

Supplementary Materials

S table 1. Materials and purchase information.

Name of Material/ Equipment	Company	Catalog Number	Comments/Description
GeneElute HP plasmid Maxiprep kit	Sigma	NA0310-1KT	
UV-vis spectrophotometer	Nanodrop	ND-1000	
Himalaya barley grains	/	/	A variety of hulless barley (store in the dark at 4° C)
Sodium succinate	Sigma	S2378	Reagent for Imbibing Solution
Calcium chloride (dihydrate)	Fisher	C79-500	Reagent for Imbibing Solution
Imbibing Solution	home made	/	20 mM sodium succinate, 20 mM calcium chloride, pH 5.0. Sterilize by autoclaving before use.
Chloramphenicol	Sigma	C0378	Prepare a 10 mg/mL stock solution in 70% ethanol.
Vermiculite	Fisher	NC0430369	Used for vermiculite plates.
Filter paper circles (90 mm)	Whatman	1001 090	Used for vermiculite and for pre-bombardment grain preparation
Vermiculite Plates	home made	/	Add 50 mL of vermiculite to a glass petri dish. Place a 90 mm paper circle on top of the vermiculite. Autoclave.
forceps (fine pointed)	Fisher	13-812-42	Used for removing seed coat from barley grains.
Forceps (ultra fine point)	Fisher	12-000-122	Used for removing seed coat from barley grains.
Gibberellin	Sigma	48870 SIGMA	Prepare 1 mM GA (0.007 g in 20 mL of 10% ethanol, freeze 1 mL aliquots)
Gold microcarriers (1.6 µm)	BioRad	1652264	
Macrocarriers	BioRad	1652335	
Calcium chloride (dihydrate)	Fisher	C79-500	Prepare a 2.5 M stock solution and store 1 mL aliquots at -20° C.
Spermidine	Sigma	S0266	Prepare a 100 mM stock solution and store 500 µL aliquots at -20° C (use within 2 months).
Rupture discs (1550 psi)	BioRad	1652331	
Stopping screens	BioRad	1652336	
Macrocarrier holders	BioRad	1652322	
Biolistic particle delivery system	BioRad	PDS-1000/He	
5-mm stainless steel beads	Qiagen	69989	
Sodium phosphate monobasic monohydrate	Sigma	S9638	Reagent for 1M sodium phosphate pH 7.2
Sodium phosphate dibasic	Sigma	S9763	Reagent for 1M sodium phosphate pH 7.2
1M sodium phosphate pH 7.2	home made	/	Combine 6.9 g of sodium phosphate monobasic monohydrate with 7.1 g of sodium phosphate dibasic. Add water to 100 mL. Add NaOH to get pH 7.2.
Dithiothrietol (DTT)	Sigma	43819	Dissolve in water to 1 M. Store at -20° in 1 mL aliquots.
Leupeptin	Sigma	L2884	Dissolve in water to 10 mg/mL. Store at -20° C.
Glycerol	Sigma	G5516	Prepare a 50% solution in water.
Grinding Buffer	home made	/	Combine 10 mL of 1 M sodium phosphate pH 7.2, 500 µL of 1 M DTT, 100 µL of 10 mg/mL leupeptin, and 40 mL of 50% glycerol. Add water to 100 mL.
Stainlesss steel beads (5 mm)	Qiagen	69989	
2.0 mL tubes	Eppendorf	22363352	This specific model of tube is recommended for use with the homogenizer.
Bead homogenizer (TissueLyser)	Qiagen	85210	
12mm x 75 mm glass test tubes	Fisher		
Luciferin	Goldbio	LUCK-100	Prepare a 25 mM stock solution and store 1 mL aliquots at -20° C.
ATP	Sigma	A7699	Prepare a 100 mM stock solution and store 250 µL aliquots at -20° C.
Tris base	Sigma	T1503	Reagent for 1M Tris sulfate pH 7.7.
Sulfuric acid	Sigma	258105	Reagent for 1M Tris sulfate pH 7.7.
1M Tris sulfate pH 7.7	home made	/	Dissolve 12.1 g Tris base in 100 mL of water. Adjust pH to 7.7 with sulfuric acid.
Magnesium chloride	Sigma	M9397	Dissolve in water to 2 M.
Luciferase Assay Buffer (LAB)	home made	/	Combine 3 mL of 1 M Tris sulfate pH 7.7, 500 µL of 2 M magnesium chloride, 1 mL of 1 M DTT, and 200 µL of 0.5 M EDTA. Add water to 50 mL.
Luciferase Assay Mixture	home made	/	Combine 15 mL of LAB, 800 µL of 25 mM luciferin, 200 µL of 100 mM ATP, and 4 mL of water. This makes enough assay mixture (20 mL) for 100 luciferase assays.
Luminometer (Sirius)	Berthold	/	
4-methylumbelliferyl-β-D-glucuronide (MUG)	Goldbio	MUG1	Dissolve in DMSO to 100 mM.
Sodium azide	Sigma	S8032	Prepare a 2% stock solution in water and store 1 mL aliquots at -20° C.
96 well plates (standard)	Fisher	12565501	
GUS assay buffer	home made	/	Combine 2.5 mL of MUG, 5 mL of 1 M sodium phosphate pH 7.2, 400 µL of 0.5 M EDTA, 1 mL of 1 M DTT, 100 µL of 10 mg/ml leupeptin, 20 mL of methanol, and 1 mL of 2% sodium azide. Add water to 100 mL.
TempPlate sealing film	USA Scientific	2921-1000	
96 well plates (black)	Costar	3916	
Sodium carbonate	Sigma	S7795	Prepare a 200 mM solution in water.
4-methylumbelliferone	Sigma	M1381	Prepare a 100 µM solution in water. Freeze 1 mL aliquots at -20° C.
Microplate fluouresence reader	Bio-Tek	FLX-800	
IPTG	Sigma	I6758-5G	
ProBond™ Purification System	ThermoFisher	K850-01	
Guanidine hydrochloride	Sigma	G4505	
Sodium Chloride	Sigma	S3014-500G	
PVPP	Sigma	P6755	
PMSF	Sigma	329-98-6	
Protease Inhibitor Cocktail	Sigma	P9599	
Phosphatase Inhibitor Cocktail 1	Sigma	P2850	
Phosphatase Inhibitor Cocktail 3	Sigma	P0044	
Phosphatase Inhibitor Cocktail 2	Sigma	P5726	
BioRad Protein assay	Bio-Rad	500-0006	
0.45 µm syringe filter units	ThermoFisher	726-2545	
10,000 MWCO centrifugal filter tubes	Millipore Sigma	UFC801024	
Formic acid	Sigma	F0507-100ml	
Ammonium hydroxide	Sigma	221228	
SDS-PAGE gel	ThermoFisher	NP0301BOX	
Imperial Protein Stain	ThermoFisher	24615	
Spectra protein marker	ThermoFisher	26634	